

Development of the metrology and imaging of cellulose nanocrystals

This article has been downloaded from IOPscience. Please scroll down to see the full text article.

2011 Meas. Sci. Technol. 22 024005

(<http://iopscience.iop.org/0957-0233/22/2/024005>)

View [the table of contents for this issue](#), or go to the [journal homepage](#) for more

Download details:

IP Address: 129.6.97.37

The article was downloaded on 05/01/2011 at 18:32

Please note that [terms and conditions apply](#).

Development of the metrology and imaging of cellulose nanocrystals

Michael T Postek^{1,4}, András Vladár¹, John Dagata¹, Natalia Farkas¹,
Bin Ming¹, Ryan Wagner², Arvind Raman², Robert J Moon^{2,3},
Ronald Sabo³, Theodore H Wegner³ and James Beecher³

¹ National Institute of Standards and Technology^{5,6}, Gaithersburg, MD 20899, USA

² Birck Nanotechnology Center, Purdue University, West Lafayette, IN 47907, USA

³ USDA Forest Service, Forest Products Laboratory, Madison, WI 53726-2398, USA

E-mail: postek@nist.gov

Received 7 April 2010, in final form 24 August 2010

Published 21 December 2010

Online at stacks.iop.org/MST/22/024005

Abstract

The development of metrology for nanoparticles is a significant challenge. Cellulose nanocrystals (CNCs) are one group of nanoparticles that have high potential economic value but present substantial challenges to the development of the measurement science. Even the largest trees owe their strength to this newly appreciated class of nanomaterials. Cellulose is the world's most abundant natural, renewable, biodegradable polymer. Cellulose occurs as whisker-like microfibrils that are biosynthesized and deposited in plant material in a continuous fashion. The nanocrystals are isolated by hydrolyzing away the amorphous segments leaving the acid resistant crystalline fragments. Therefore, the basic raw material for new nanomaterial products already abounds in nature and is available to be utilized in an array of future materials. However, commercialization requires the development of efficient manufacturing processes and nanometrology to monitor quality. This paper discusses some of the instrumentation, metrology and standards issues associated with the ramping up for production and use of CNCs.

Keywords: cellulose, nanofibers, nanocrystal, microscopy, standards, metrology, measurement

1. Introduction

Biomass surrounds us from the smallest alga to the largest redwood tree. Even the largest of trees owes its strength to a newly appreciated class of nanomaterials known as cellulose nanocrystals (CNCs). Cellulose is the world's most abundant polymer and, as such, is renewable and biodegradable. CNCs occur as whisker-like microfibrils that are biosynthesized and deposited in plant material in a continuous fashion. CNCs are also produced by

certain bacteria and some small sea animals [1]. As shown in figure 1, in wood, these CNCs are hierarchically structured into a macroscopic cellular biocomposite made up of cellulose, hemicellulose, lignin, extractives and trace elements [2]. Therefore, the basic raw materials for a future of new nanomaterials already abound in the environment, are being assembled into macroscale structures, and will be commercially available once the nanometrology and viable manufacturing processes are developed. Lignocellulosic fibers derived from sustainable, renewable resources such as wood used as a reinforcing phase in polymeric matrix composites provide positive environmental benefits with respect to biodegradability and the energetic cost of production.

However, accurate measurements associated with chemical, dimensional and structural characteristics must be developed for the full commercial exploitation of this material. Metrology and imaging of these cellulose-based nanomaterials

⁴ Author to whom any correspondence should be addressed.

⁵ Contribution of the National Institute of Standards and Technology; not subject to copyright.

⁶ Certain commercial equipment is identified in this report to adequately describe the experimental procedure. Such identification does not imply recommendation or endorsement by the National Institute of Standards and Technology, nor does it imply that the equipment identified is necessarily the best available for the purpose.

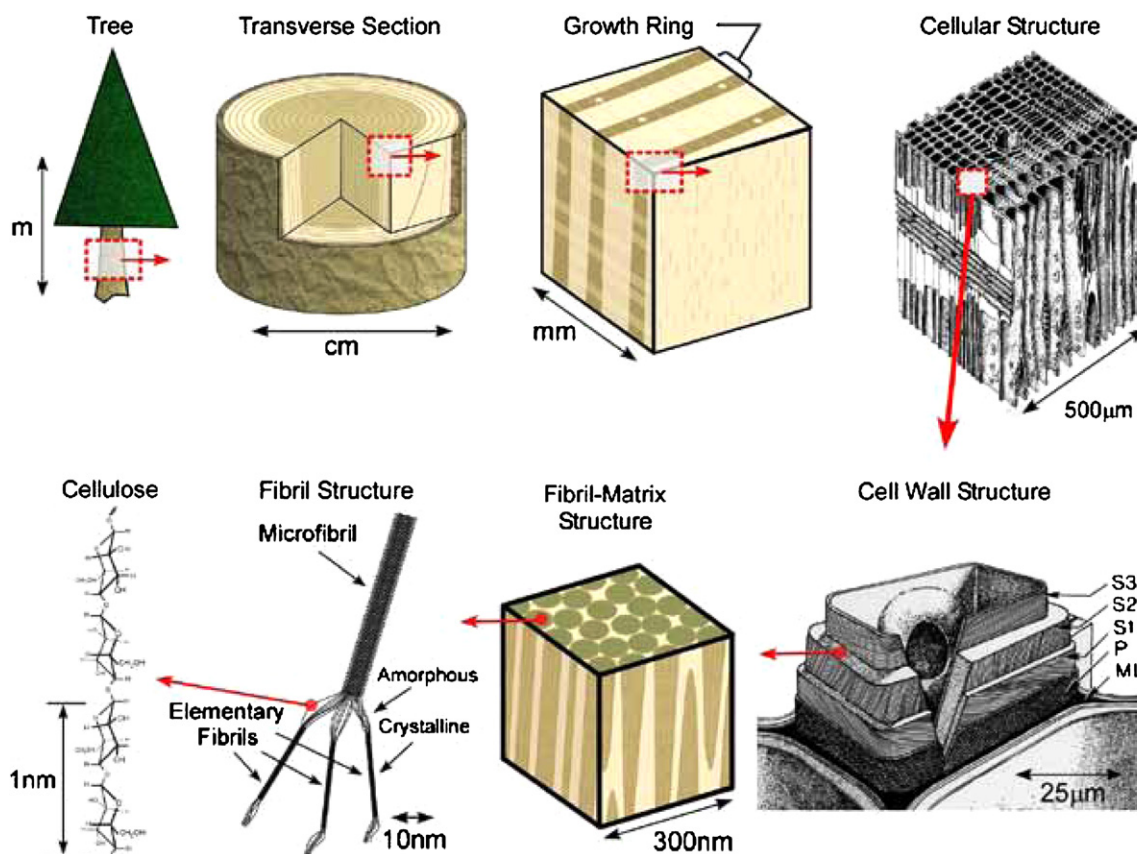


Figure 1. Structure of wood from the tree to the CNCs (after [2]). ML = middle lamellae between tracheids, P = primary cell wall, S1, S2, S3 = cell wall layers.

are critical components in the value-added manufacturing chain from discovery of nanomaterials to commercialization of nano-enabled products. The immediate tasks at hand are to develop protocols and adapt currently available nanoscale metrology and instrumentation to biological nanodimensional materials to obtain artifact-free property measurements. Instrumentation to probe the nanoscale and to adapt instrumentation to biological materials oftentimes require both evolutionary and revolutionary developments and advances in measurement schemes and instruments.

1.1. Cellulose nanocrystals

Natural fibers are pervasive throughout the world in plants such as grasses, reeds, stalks, woody vegetation, certain bacteria and some small marine animals. Liberating nanomaterials from plants involves processing to disaggregate various constitutive materials and architectures. For wood (figure 1), this involves separation of wood into individual tracheids, vessel elements and parenchyma cells along with the removal of lignin and hemicelluloses [2]. Wood is about 30–40% cellulose with about half in nanocrystalline form and half in amorphous form. Individual CNCs are of crystalline form and are typically 2–6 nm wide and hundreds of nanometers long. Individual CNCs are composed of both crystalline and amorphous regions and can be hundreds to thousands of nanometers long. In addition, CNCs can be in various levels of aggregation making them tens

of nanometers wide or more. Plant material is most commonly processed using chemical action employed in wood pulping to remove first the hemicelluloses and lignins leaving cellulose fiber. The resulting cellulosic fibers are then further processed to liberate CNCs and nanocrystals using mechanical action and strong acids or enzymes. By manipulating the processing, microfibrillar, nanofibrillar and CNCs can all be produced as desired.

Recent research suggests that these agro-based fibers are a potentially, viable alternative to inorganic/mineral-based reinforcing fibers in commodity fiber thermoplastic composite materials [3]. Research has shown that ‘by adding one ounce of crystals (of cellulose) to a pound of plastic, you can increase the strength of the plastic by a factor of 3000’ [4]. A routine problem encountered with such additives is that the polymer materials often becomes brittle, implying a sharp reduction in the amount of deformation possible before breaking. This can render the nanocomposite of limited practical use. Yet, much research needs to be done especially in the areas of dispersion and the accuracy of the measurements. A similar issue has been encountered with carbon nanotubes, which are of commercial interest mainly because of their potential structural and electrical conductivity properties. Thus far, mechanical property improvements have been disappointing in these materials despite the hype made about the potential of these additives. The expectation is that, where CNCs are concerned, the more compliant and more

chemically compatible nanoparticle properties are relative to the polymer matrix, the more successful the CNC additives will become. In addition, biological systems provide the potential for genetic modification of the manufacturing location (the plant). Irrespective of the source, reliable measurement methods for the geometrical and mechanical properties of the CNCs are required to explore the potential of these materials in a meaningful way.

Plants contain a minimum of about 25% cellulose, and this material can and has been harvested for many purposes. Pulp and paper manufacturing is the main and most obvious product. In addition, micro-dimensional crystalline cellulose particles are currently used as an industrial processing aid. These particles are included in numerous pharmaceutical and food products. Therefore, their biocompatibility has already been demonstrated. Commercially available cellulose particles are commonly referred to as microcrystalline cellulose and typically consist of micrometer sized particles. However, the use of nanometer sized particles (i.e. CNCs) is expected to become more widespread because of the advantages that these nanoparticles can offer over micron-sized particles. For example, CNCs are composed of nearly 100% crystalline cellulose, providing greater stiffness and higher tensile strengths than the wood fibers that have traditionally been used. Because of their small size, high aspect ratios, high stiffness and remarkable strength, CNCs are a logical choice for reinforcing polymer materials.

Researchers at the Department of Energy Pacific Northwest National Laboratory [5] have recently reported the use of CNCs as templates to grow unique metal nanoparticles that show promise for use in biosensors, catalysis and photovoltaics. Examples for growing metal particles using CNC templates include a method for producing novel porous titania materials [6] and a simple 'green' method for preparing nickel [7] and selenium nanoparticles [8]. Additionally, cationic surfactants have been used to promote preferential room temperature precipitation of fine dispersions of metallic (silver, gold, copper or platinum) [9] or semiconducting (cadmium sulfide, zinc sulfide and lead sulfide) [10] particles that are strongly bonded to individual CNCs.

1.2. Metrology challenges

It is well known that accurate dimensional metrology and characterization of nanomaterials for nanomanufacturing remain a problematical issue [11]. One of the leading candidates, carbon nanotubes (CNTs), has received considerable attention because it has been touted as one of the most promising of the nanomaterials for commercial manufacturing. However, in most instances, nanomanufacturing processes for CNTs remain little more than expanded laboratory experiments, the measurement techniques are still evolving, and reproducible manufacturing methods are, only now, beginning to appear. More importantly for the CNT and other allied nanoparticles, the potential toxicity is being debated [12, 13] and has not been fully documented in the literature [14]. In addition, where CNT are concerned, the life-cycle fate of the nanoparticles is

unknown for CNT-reinforced products, whereas CNCs can potentially degrade (under appropriate conditions) to carbon dioxide and water within 90 days [4]. Alternatively, CNCs have the potential: (1) to be as useful as CNTs for many applications; (2) to have no toxic components; (3) to have established manufacturing processes; (4) to be renewable; and (5) are generally biologically compatible. But, a whole host of measurement methodologies are needed to prove the value of these materials, specimen preparation techniques need to be adapted and qualified and new polymer formulations need to be tested.

2. Materials and methods

CNCs were imaged with the scanning electron microscope (SEM), helium ion microscope (HIM), and scanned probe microscope (SPM). Aqueous suspensions of CNCs were prepared by the acid hydrolysis of woody materials with sulfuric acid [15]. The material used for imaging in this preliminary study was obtained from the United States Department of Agriculture (USDA) Forest Service, Forest Products Laboratory. Typically, the as-received CNC suspensions were diluted using deionized water (1:100), a 20 μ l droplet of the CNC solution was then deposited onto a freshly cleaved mica or poly-L-lysine (PLL)-coated mica disk (see below) and incubated for 1 min. The sample was immersed in water to remove unattached CNCs. Samples were then blown dry for dry imaging, or maintained under water for fluid imaging. The treated mica disks were then mounted on a steel disk sample holder. Additional imaging was carried out on freeze-dried material mounted directly on the sample holders and coated for the SEM, or left uncoated for the SPM and HIM.

2.1. Scanning electron microscopy

Samples for the SEM observation were either observed uncoated at low accelerating voltage or with a light osmium tetroxide coating. The SEM was done using an FEI Company⁶ thermal field emission SEM using secondary electron collection.

2.2. Helium ion microscopy

Samples for the HIM were mounted as above, but were generally viewed uncoated. The HIM was done using a Zeiss/ALIS Orion⁶ HIM using secondary electron collection. The electron flood gun was used to eliminate the charge build-up on the sample.

2.3. Scanning probe microscopy

SPM fluid imaging was performed with a Veeco MultiMode AFM and a Nanoscope IV controller⁶. Nanoscope Version 6 software was used for data acquisition. Dry imaging was performed in TappingMode using Veeco model OTESP cantilevers. For fluid imaging, a TappingMode fluid cell, without an O-ring, and Veeco model OTR8 'B' cantilevers (24 kHz nominal resonance frequency in air) were used for

fluid imaging by oscillating the cantilever in the low-frequency acoustic mode region, about 7 to 9 kHz.

2.4. Elastic properties

SPM elastic property measurements were performed with a Nanotec⁶ AFM and Dulemia controller (Tres Cantos, Spain). WSxM software version 4.0 Develop 13.0 [16] was used for data collection and analysis. Force–displacement (*FZ*) curves [17] were collected under dry conditions (0.1% relative humidity) on isolated tunicate-derived CNCs [18] deposited on freshly cleaved mica. Details of the tunicate CNC preparation method are given in van den Berg *et al* 2007 [18]. The *FZ* curves were first converted into force–distance (*FD*) curves, then the Hertz-based DMT model [19] was used to convert the *FD* data into an elastic modulus [20] systematically since this model accounts for the measured adhesion forces also. The mica was not coated with PLL to avoid the potential of adding a soft thin film to the surface that could influence the elastic measurements. AppNano FORT⁶ force modulation cantilevers (AppNano.com) with a nominal spring constant of 3 N m^{-1} and resonance frequency of 62 kHz were used for imaging. The individual stiffness of each cantilever was calibrated with the thermal tuning method [21]. The force curves were mapped over an 800 nm by 800 nm region with a displacement of 60 nm with a maximum force of 30 nN. Data points were selectively analyzed from the ‘apex’ of the CNC crystal. For more details see [22].

2.5. Substrate preparation for imaging

A freshly cleaved mica substrate is immersed in a 0.01 PLL solution diluted from 0.1% weight-to-volume stock solution (Sigma-Aldrich) for 30 min and blown dry.

3. Results

3.1. Aqueous CNC material

Hydrolysis parameters—such as plant or animal starting material, reaction time, processing temperature, acid to pulp ratio and type of acid used—affect the size and size distribution of the CNCs and the degree of aggregation of the suspension. Precise knowledge of the size and morphology of the CNCs is needed to facilitate product development and provide quality control for manufacturing. Size, polydispersity, morphology of the CNC and aggregation and particle-density of suspension are key properties determining the functionality and prospective application of the material. Despite the established manufacturing processes for cellulose fibers, the lack of measurement methodologies hinders their potential use for a wide range of commercial applications.

Size measurements of the CNC are usually conducted by microscopy or light scattering techniques and are generally problematic. Commonly reported practice is to use different methods to determine the width and the height of the CNC such as SEM, transmission electron microscope (TEM) and SPM respectively [23]. Consequently, comprehensive size

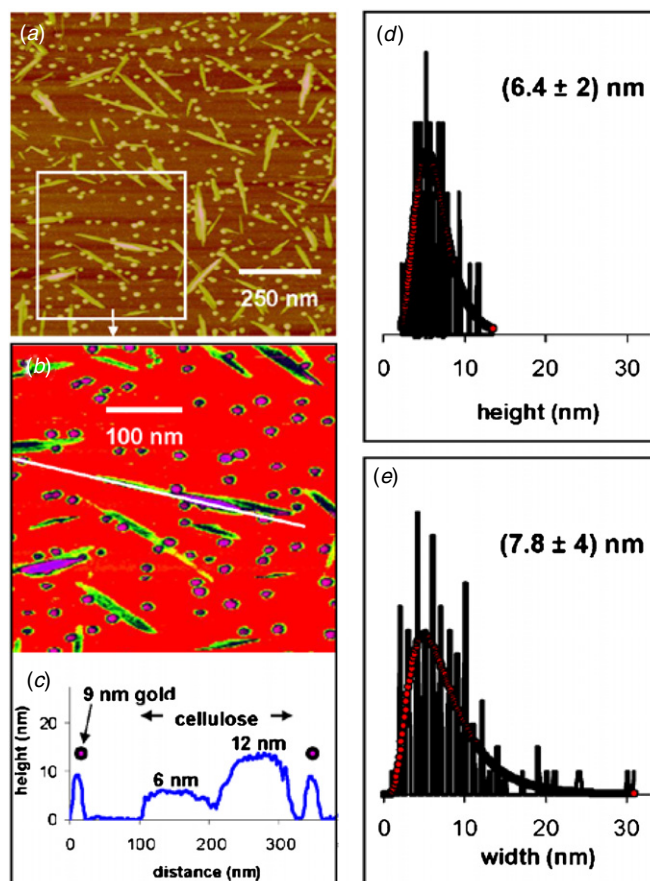


Figure 2. (a) SPM fluid image of CNCs co-adsorbed with citrate-stabilized gold nanoparticles with 10 nm nominal diameter. (b) Higher magnification false-colored image showing the broad size distribution of CNCs against the monodisperse gold nanoparticles serving as an *in situ* height reference. (c) Topographic cross-section of a CNC aggregates lengthwise next to two reference gold nanoparticles. (d) SPM height distribution of CNC with a mean height of 6.4 nm. (e) SPM width distribution of CNC after correction for tip convolution with a mean width of 7.8 nm. The number of CNCs analyzed was 100. The tip diameter is obtained from size measurements of the gold reference particles. The open circles represent a log-normal distribution least-squares fit to the data.

descriptions of CNCs are limited as different techniques have intrinsically different limitations and thus the measurements may vary. SPM width measurement is inaccurate because of SPM tip broadening so the height of the CNC is measured, with the assumption that the nanocrystals are cylindrical in cross-section. Sample preparation plays an important role since highly aggregated nanocrystals make size measurements inconclusive as side-by-side and end-to-end twinning are not always obvious and the sampling may not be statistically unbiased when only a few isolated CNCs are measured and included in the size analysis.

In the present study, SPM imaging was utilized to characterize CNCs and the above-mentioned measurement challenges are addressed by developing sample-specific substrate preparation methods and the use of *in situ* tip calibration standards.

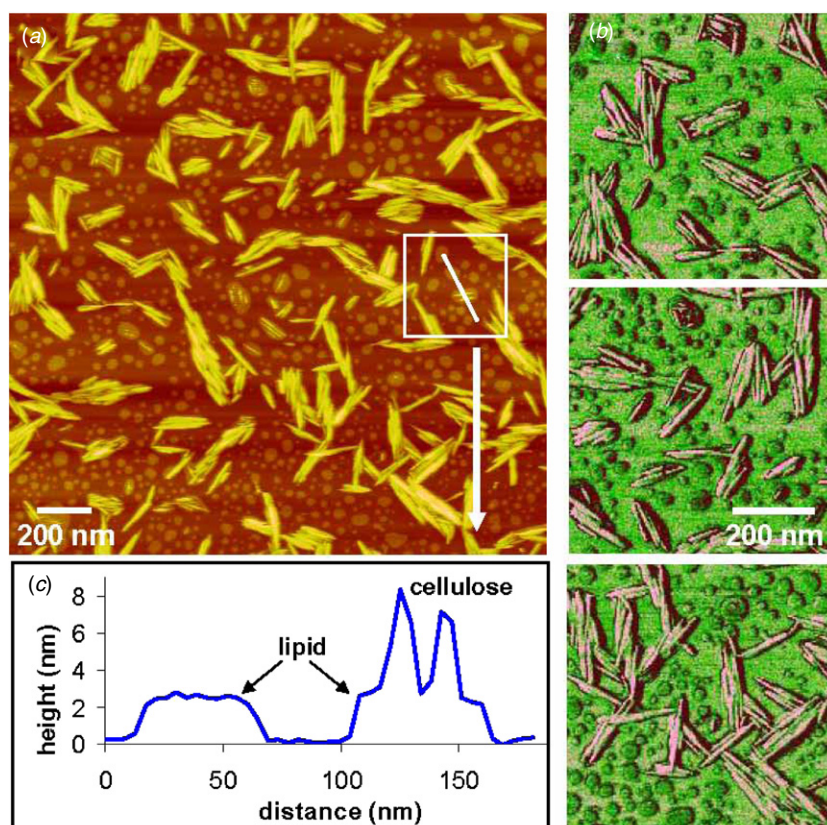


Figure 3. (a) Fluid SPM image of individual CNCs organized on surface chemically modified mica. (b) High magnification SPM phase images of closely packed individual CNC aligned parallel next to each other. (c) Topographic cross-section of the CNC–lipid multilayer structure.

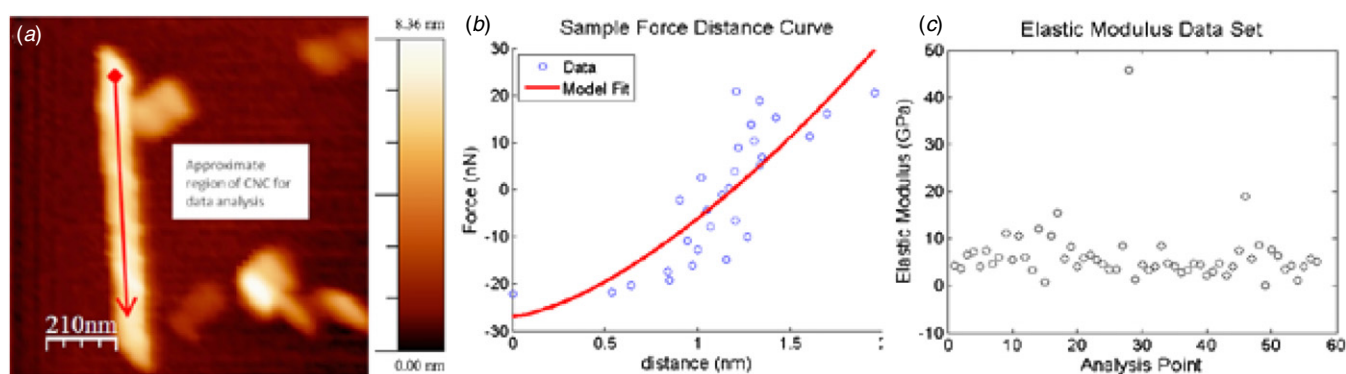


Figure 4. (a) SPM topography image of an isolated tunicate CNC chosen for analysis. (b) One of the 56 FZ curves extracted from CNC, with the corresponding curve fit based on the DMT contact mechanics model on a cylinder used for modulus estimation. (c) Elastic modulus data set for the 56 FZ measurements.

CNCs need to be immobilized after being dispersed on a substrate for both high-resolution SPM imaging and statistical size measurements. The adsorption properties of the CNC onto a solid surface are determined mainly by electrostatic interaction. An essential first step in sample preparation therefore involves matching the zeta potential of CNCs in solution to the zeta potential of the substrate surface. The nanocrystals are negatively charged as a result of hydrolysis using sulfuric acid, so the obvious choice of a substrate is PLL-coated mica that has a highly positive charge when it is freshly prepared.

In order to implement *in situ* tip calibration, citrate-stabilized gold reference particles—NIST Reference Material 8011 [24]—having a 10 nm nominal diameter are co-adsorbed with the CNCs. The size of the gold particles was chosen to be comparable to that of the CNCs. The presence of particles with the known geometry and considerably narrow size distribution allows correction for tip convolution and provides *in situ* imaging control under fluid SPM conditions.

Figure 2(a) shows a fluid SPM image of the CNC and gold nanoparticles co-adsorbed on PLL-coated mica. By optimizing the concentration and incubation conditions for

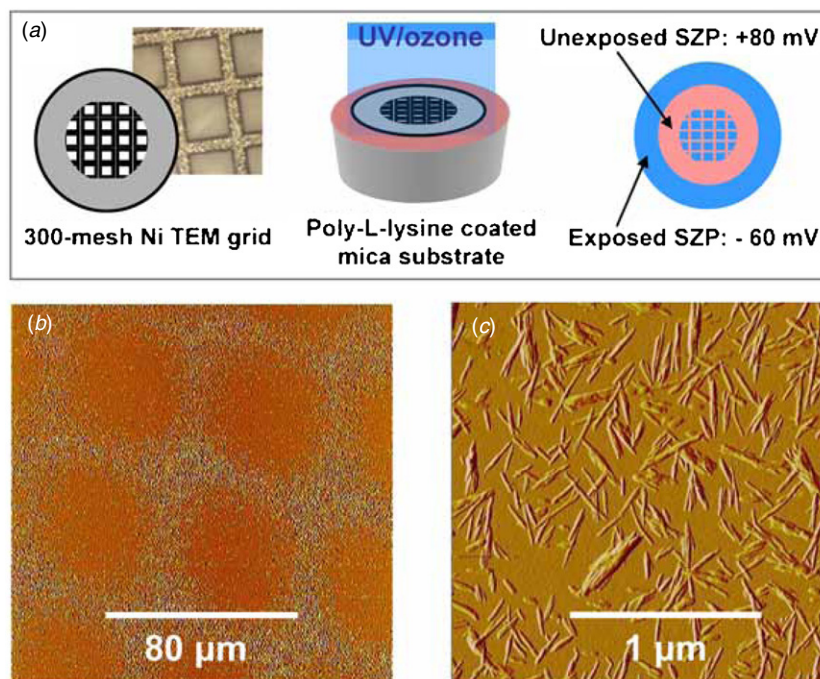


Figure 5. Selective adsorption of CNCs on an SZP patterned PLL-coated mica. (a) Schematic of the SZP patterning technique. (b) Dry SPM amplitude image of the CNC pattern. (c) Higher magnification SPM amplitude image of CNCs adsorbed on the unexposed, therefore positively charged, region of the pattern.

both the CNC and gold solutions, well-dispersed CNCs and reference nanoparticles are obtained on the surface. A higher magnification false-colored topographic image of figure 2(b) emphasizes that the size distribution of CNCs appears to be broader than that of the monodisperse spherical gold nanoparticles. Figure 2(c) presents a topographic cross-section of a CNC aggregate lengthwise next to two reference gold nanoparticles. Note that the size of the gold reference particles fall into the height range of the CNCs.

The first step of the SPM image data analysis is to obtain height and width distributions for the gold reference particles. The tip diameter is then calculated by subtracting the mean height from the mean apparent width assuming an aspect ratio of unity for spherical particles. Then we proceed with the size analysis of the CNC. Figures 2(d) and (e) provide the resulting height and width distributions of 100 CNCs, respectively. Values are reported in the form $(M + N)$ nm where M is the mean and N the standard deviation obtained from a fit to the lognormal distribution function. No adjustment is made in the case of height data, whereas the width distribution is corrected for tip convolution using tip diameter obtained from size analysis of the co-adsorbed gold reference particles. The mean corrected width of the CNCs is slightly larger than the mean height, namely 6.4 nm and 7.8 nm, respectively. The broader width distribution results from the association of individual nanocrystals to form larger aggregate structures.

The presence of particles with the known size and narrow size distribution *in situ* is crucial for the quantitative size assessment of the CNCs. The results demonstrate that SPM-based size analysis, including width measurements, are suitable and can be successfully used for CNC characterization and are applicable to other nanoparticles.

To demonstrate that chemical modification of the substrate influences the association of the CNCs upon adsorption, a layer-by-layer deposition of lipid and CNC was employed. This example demonstrates that substrate preparation not only is crucial in order to adhere particles to the surface but is also a versatile tool to control the alignment and organization of CNCs.

Freshly cleaved mica was incubated with cationic liposomes followed by a thorough wash to discard the unattached material. In this first sample preparation step, the cationic liposomes rupture and form lipid bilayer patches on the surface due to the large electrostatic interaction with the highly negative mica. Then the incubation and wash steps are repeated with a diluted CNC solution. The CNCs are immobilized on these lipid patches so that they are strongly held in place during fluid imaging. The resulting fluid SPM topographic and higher magnification phase images are shown in figures 3(a) and (b) along with a representative cross-section of the CNC–lipid multilayer system revealing the hierarchy of the CNC–lipid structure in figure 3(c).

The first to note is that the CNCs are exclusively immobilized on the cationic lipid. Secondly, individual CNCs tend to stack up in a parallel manner filling up and occasionally connecting the underlying lipid patches. As shown in figure 2 and described above, CNCs are well dispersed and oriented randomly on PLL-coated mica which is therefore proven to be a suitable substrate for SPM-based size analysis. Here, on the other hand, CNCs from the same suspension are closely packed next to each other along their long axis, better seen in the phase images of figure 3(b). This result suggests that manipulation and alignment of CNCs is possible by chemical

modification of a substrate, for example by controlling the lipid coverage.

3.2. Elastic property metrology

The isolated tunicate CNC that was characterized by the SPM indentation technique is shown in figure 4(a). For this study, 56 *FZ* curves were analyzed along the CNC length; a sample *FD* dataset and corresponding curve fit for a single indent is shown in figure 4(b), while the estimated elastic modulus for each *FZ* curve is shown in figure 4(c). For this particular tunicate CNC, and the corresponding 56 *FZ* curves that were analyzed, the resulting transverse elastic modulus has a mean of 6 GPa and a standard deviation of 6 GPa. This large standard deviation is mainly due to a few outliers in the data set shown in figure 4(c). There are several issues that need to be kept in mind while considering this mean modulus value. (1) This modulus was extracted by applying an isotropic model to a nonisotropic material. This implies that this number is not a true transverse modulus but rather a ‘model equivalent’ elastic constant that can be used for sample to sample comparison. Models that are more sophisticated need to be applied to extract true elastic constants. (2) There exists a large systematic uncertainty associated with the AFM calibration parameters and the propagation of this uncertainty through the experimental setup is complicated. This systematic uncertainty was not addressed in the measurements of the current study. Improvements can be made on the methods for collecting and analyzing elastic data on nanoscale structures; this is an ongoing work that will be presented in a subsequent paper [25].

There has been, to date, only a very limited number of studies that have attempted to measure the elastic properties of CNCs. This is a direct result of the challenges imposed due to their extremely small size. The elastic properties of individual CNCs, and bacterial cellulose particles have been measured in the axial direction, E_A [26–30], and in the transverse direction, E_T [22, 25]. The property anisotropy between the axial and transverse directions is expected based on the monoclinic crystal structure of crystalline cellulose (I_β). Axial elastic properties are typically measured using AFM atomic three-point bending of individual CNCs [27, 29], or *in situ* combination of tensile tests experiments with Raman spectroscopy of thin mats of t-CNC impregnated with epoxy [26, 28, 30]. The resulting measured axial elastic properties $E_A = 60\text{--}180$ GPa were in general agreement to model calculations of $E_A = 124\text{--}155$ GPa [31].

The transverse elastic properties have been measured using a combination of high-resolution AFM indentation and modeling [22, 25], in which individual CNCs from wood $E_T = 18\text{--}50$ GPa, and tunicate $E_T = 9 \pm 3$ GPa, respectively. These results are similar to the theoretical model calculations of $E_T = 10\text{--}57$ [32–34]. Note that there is a high probability of errors with such measurements that are associated with testing at AFM sensitivity limits, and model assumptions used to extract the mechanical properties. Additionally, the specific crystallographic direction within the transverse direction of the CNCs could not be confirmed; thus, this would also contribute to variations in property measurements.

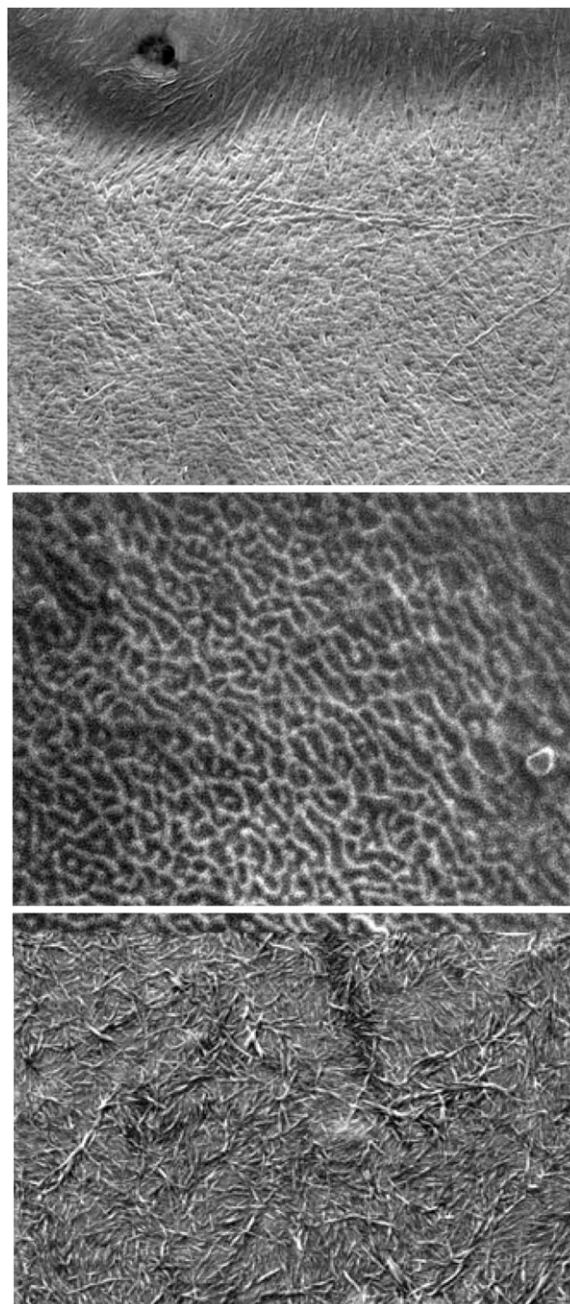


Figure 6. Particle beam microscopy. Top: scanning electron micrograph of freeze-dried CNCs which have been lightly coated with osmium tetroxide. (Field of view = $2.52\ \mu\text{m}$.) Middle: helium ion microscope image of uncoated CNCs. (Field of view = $1\ \mu\text{m}$.) Bottom: low accelerating voltage scanning electron microscopy of dispersed CNCs viewed uncoated. (Field of view = $2.22\ \mu\text{m}$.)

3.3. Zeta potential patterning

A method for application of a surface zeta potential (SZP) patterning method for PLL-coated mica has been developed for the CNCs. Specifically, the zeta potential of the PLL substrate is varied over a range of approximately -60 mV to $+100$ mV by exposure to ozone generated by ultraviolet light. SZPs are measured by the rotating disk method.

Exposure through a mask produces local regions of positive and negative surface charge on PLL-coated mica. The

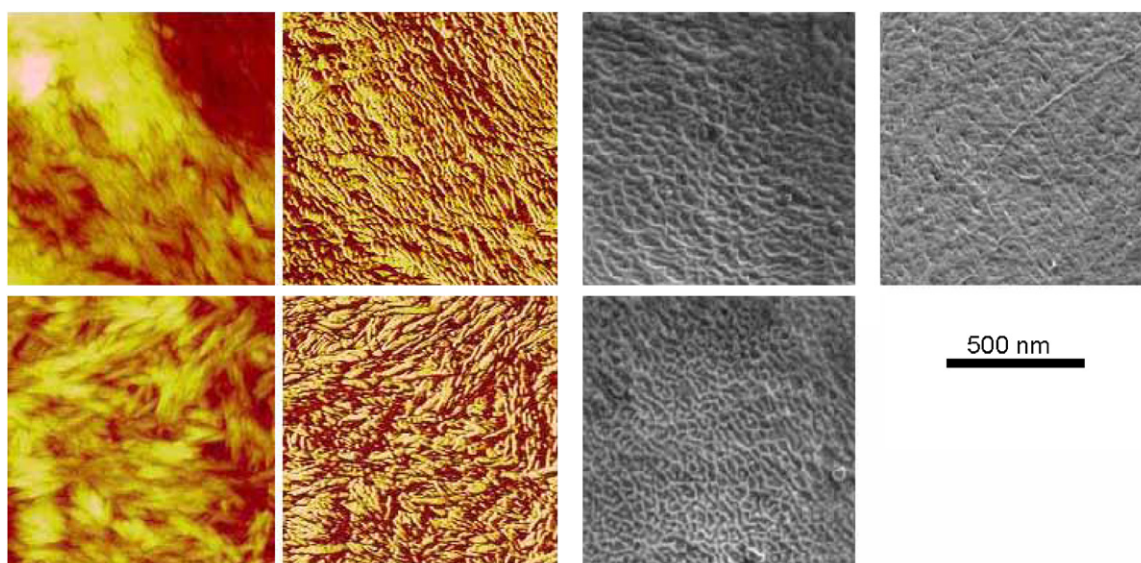


Figure 7. Comparison of the imaging of freeze-dried CNC by the SPM topography mode (left, top and bottom); SPM phase mode (left center, top and bottom), HIM (right center top and bottom) and SEM (right). The images indicate that the CNCs are relatively resilient to the sample preparation methods employed in this study and that the individual nanocrystals more readily observed when the bundles they form are parallel to the surface.

attachment of the CNC onto this SZP patterned substrate is shown in figure 5. As adsorption of CNCs is mainly driven by electrostatic interaction, they are preferentially immobilized on the unexposed and therefore positively charged area. The patterning of the CNC offers a template to assemble and study the multilayer structures of CNCs. One might imagine combining the patterning and alignment methods in succession to engineer the three-dimensional architectures of CNC building blocks as model systems for potential applications.

3.4. Air/freeze-dried material

Air-dried and freeze-dried CNCs were viewed in the AFM, SEM and HIM. The topography of the freeze-dried cellulose sheet depends on the packing and orientation of the nanocrystals. Figure 6 is an SEM micrograph of osmium-coated freeze-dried material (figure 6(a)) and HIM (figure 6(b)) images of the similar material uncoated. Figure 6(c) is a SEM micrograph of uncoated CNC material at low accelerating voltage. The differences in the imaging between the SEM and the HIM are currently being explored. Some differences between the SEM and the HIM imaging are expected due to the secondary electron generation processes and subsequent images produced (see [35] in this issue). Figure 7 is a visual comparison between the three methods employed. The topography of the freeze-dried CNCs is shown to depend upon the packaging and orientation of the nanoparticles. In particular, individual nanocrystals are seen more readily when the bundles they form are parallel to the surface. More importantly, there appears to be no apparent difference in topography and phase between individual CNCs of freeze-dried and in-solution samples. The effect of topography is less pronounced in the SPM phase image

providing a more uniform picture reflecting the collective material properties of the cellulose sheet.

Therefore SPM phase images resemble more the HIM and SEM images where the network-like appearance shows collective properties rather than the topography of the CNCs (figure 7).

4. Conclusions

In this study, CNCs have been successfully viewed with the SEM, HIM and SPM and initial measurements made. Suitable sample preparation steps have been developed and the differences between air-dried, aqueous and freeze-dried material have been evaluated to assess the potential for artifact formation. The results demonstrate that these instruments may be used for dimensional metrology and size analysis, including width measurements, and are thus suitable and can be successfully used for CNC characterization. The CNCs are able to be well dispersed and oriented randomly on PLL-coated mica which has proven to be a suitable substrate for size analysis. Elazzouzi–Hafraoui *et al* [23] attempted to determine height with the AFM, but they felt the results were inconclusive because of the difficulties dispersing the CNCs. The methods described here demonstrate that this issue can be substantially improved. The results also suggest that manipulation and alignment of CNCs is possible by chemical modification of a substrate, for example by controlling the lipid coverage.

A SPM nanoindentation technique was used to measure the transverse elastic modulus of an individual tunicate CNC at multiple locations. Quantitative mechanical property measurements are problematic for such small particles as measurement uncertainty is amplified because displacement measurements are near the SPM sensitivity limits and assumptions used in contact models for property extraction

are extensive. Great care must be taken when reporting mechanical properties from such measurements as more work is needed to understand the propagation of uncertainty.

CNCs should be explored further as a suitable alternative to CNTs as reinforcing materials for appropriate applications. Recent publications on environmental, health and safety (EHS) issues related to use of nanomaterials such as CNTs in the scientific and popular press have generated general public concern about nanomaterials. CNTs, which have been highly studied, are now beginning to be more highly scrutinized with respect to undesirable EHS impacts whereas microcrystalline cellulose has been utilized as fillers in pharmaceuticals for many years with no known detrimental biological responses. The value of CNCs as an alternative to CNTs or as a co-constitutive material with CNTs in various applications has yet to be determined, but only further work on these new materials and the development of accurate metrology will be able to tell for sure.

Acknowledgments

The authors would like to thank US Forest Service and Purdue University for partially funding this project. They are grateful to Professors Jeff Capadona and Stuart Rowan from Case Western University and Christoph Weder from the University of Fribourg, Switzerland for providing the tunicate CNCs used in the SPM nanomechanics testing.

References

- [1] Samir M A S A, Alloin F and Dufresne A 2005 Review of recent research into cellulosic whiskers, their properties and their application in nanocomposite field *Biomacromolecules* **6** 612–26
- [2] Moon R J 2008 *Nanomaterials in the Forest Products Industry* (Chicago, IL: McGraw-Hill) pp 226–9
- [3] Favier V, Canova G R, Cavaille J-Y, Chanzy H, Dufresne A and Gauthier C 1995 Nanocomposites materials from latex and cellulose whiskers *Polym. Adv. Technol.* **6** 351–5
- [4] Winter W 2008 Cellulose nanocrystals make plastic 3000 times stronger *Nanowerk News* <http://www.nanowerk.com/news/newsid=933.php>
- [5] Shin Y, Yao C, Risen W M and Exarhos G J 2007a Controlled formation of colloidal carbon spheres with core-shell structures from cellulose *American Chemical Society Spring Meeting (Chicago, IL, 27 March 2007)* <http://www.pnl.gov/science/highlights/highlight.asp?id=149>
- [6] Shin Y and Exarhos G 2007 Template synthesis of porous titania using cellulose nanocrystals *Mater. Lett.* **61** 2594–7
- [7] Shin Y, Bae I, Arey B W and Exarhos G 2007b Simple preparation and stabilization of nickel nanocrystals on cellulose nanocrystal *Mater. Lett.* **61** 3215–7
- [8] Shin Y, Blackwood J, Bae I, Arey B and Exarhos G 2007c Synthesis and stabilization of selenium nanoparticles on cellulose nanocrystal *Mater. Lett.* **61** 4297–300
- [9] Padalkar S, Capadona J, Rowan S, Weder C, Stanciu L and Moon R J 2010 Natural biopolymers: novel templates for the synthesis of nanostructures *Langmuir* **26** 8497–502
- [10] Padalkar S, Capadona J, Rowan S, Weder C, Stanciu L and Moon R J 2010 Cellulose assisted synthesis of semiconductor nanowires *J. Mater. Chem.* submitted
- [11] Postek M T and Lyons K 2007 Instrumentation, metrology, and standards key elements for the future of nanomanufacturing *Proc. SPIE* **6648** 664802
- [12] Poland C, Duffin R, Kinloch A, Maynard A, Wallace W, Seaton A, Stone V, Brown S, MacNee W and Donaldson K 2008 Carbon nanotubes introduced into the abdominal cavity of mice show asbestos-like pathogenicity in a pilot study *Nature Nanotechnol.* www.nature.com/nanotechnology
- [13] Murashov V 2008 Should carbon nanotubes be handled in the workplace like asbestos? NIOSH Science Blog http://www.cdc.gov/niosh/blog/nsb052008_nano.html
- [14] Berube D 2008 Rhetorical gamesmanship in the nano debates over sunscreens and nanoparticles *J. Nanopart. Res.* **10** 23–37
- [15] Revol J-F, Bradford H, Giasson H, Marchessault R and Gray D 1992 Helicoidal self-ordering of cellulose microfibrils in aqueous suspension *J. Biol. Macromol.* **14** 170–2
- [16] Horcas I, Fernandez R, Gomez-Rodriguez J, Colchero J, Gomez-Herrero J and Baro A 2007 WSXM: a software for scanning probe microscopy and a tool for nanotechnology *Rev. Sci. Instrum.* **78** 013705
- [17] Butt H, Cappella B and Kappl M 2005 Force measurements with the atomic force microscope: technique, interpretation and applications *Surf. Sci. Rep.* **59** 1–152
- [18] Van Den Berg O, Capadona J R and Weder C 2007 Preparation of homogenous dispersions of tunicate cellulose whiskers in organic solvents *Biomacromolecules* **8** 1353–7
- [19] Derjaguin B, Muller V and Toporov Y 1975 Effect of contact deformations on the adhesion of particles *J. Colloid Interface Sci.* **53** 314–26
- [20] Wagner R, Raman A and Moon R 2009 Transverse elasticity of cellulose nanocrystals via atomic force microscopy *10th Int. Conf. on Wood & Biofiber Plastic Composites and Cellulose Nanocomposites Symp. (Madison, WI, Forest Products Society, 11–13 May 2009)* pp 309–16
- [21] Butt H and Jaschke M 1995 Calculation of thermal noise in atomic force microscopy *Nanotechnology* **6** 1–7
- [22] Lahiji R, Xu X, Reifengerger R, Raman A, Rudie A and Moon R 2010 Atomic force microscopy characterization of cellulose nanocrystals *Langmuir* **26** 4480–8
- [23] Elazzouzi-Hafraoui S, Nishiyama Y, Putaux J-L, Heux L, Dubreuil F and Rochas C 1980 The shape and size distribution of crystalline nanoparticles prepared by acid hydrolysis of native cellulose *Biomacromolecules* **9** 57–65
- [24] Reference Material 8011 https://www-s.nist.gov/srmors/view_detail.cfm?srm=8011
- [25] Wagner R, Moon R, Pratt J, Shaw G and Raman A 2010 Uncertainty quantification in nanomechanical measurements using the atomic force microscope, in preparation
- [26] Šturcová A, Davies G R and Eichhorn S J 2005 Elastic modulus and stress-transfer properties of tunicate cellulose whiskers *Biomacromolecules* **6** 1055–61
- [27] Guhados G, Wan W and Hutter J L 2005 Measurement of the elastic modulus of single bacterial cellulose fibers using atomic force microscopy *Langmuir* **21** 6642–6
- [28] Hsieh Y-C, Yano H, Nogi M and Eichhorn S J 2008 An estimation of the Young's modulus of bacterial cellulose filaments *Cellulose* **15** 507–13
- [29] Iwamoto S, Kai W, Lsogai A and Iwata T 2009 Elastic modulus of single cellulose microfibrils from tunicate measured by atomic force microscopy *Biomacromolecules* **10** 2571–6
- [30] Rusli R and Eichhorn S J 2008 Determination of the stiffness of cellulose nanowhiskers and the fiber-matrix interface in a nanocomposite using Raman spectroscopy *Appl. Phys. Lett.* **93** 033111

- [31] Tanaka F and Iwata T 2006 Estimation of the elastic modulus of cellulose crystal by molecular mechanics simulations *Cellulose* **13** 509–17
- [32] Jaswon M A, Cillis P P and Mark R E 1968 The elastic constants of crystalline native cellulose *Proc. R. Soc. A* **306** 389–412
- [33] Tashiro K and Kobayashi M 1991 Theoretical evaluation of three-dimensional elastic constants of native and regenerated celluloses: role of hydrogen bonds *Polymer* **32** 1516–26
- [34] Jaswon M A, Cillis P P and Mark R E 1968 The elastic constants of crystalline native cellulose *Proc. R. Soc. A* **306** 389–412
- [35] Postek M T, Vladár A, Archie C and Ming B 2010 Review of current progress in nanometrology with the helium ion microscope *Meas. Sci. Technol.* **22** 024004